Int. J. Dev. Biol. 65: 301-311 (2021)
https://doi.org/10.1387/ijdb.200080np

THE INTERNATIONAL JOURNAL OF DEVELOPMENTAL BIOLOGY
www.intjdevbiol.com

Anatomical and genetic bases underlying the convergent evolution of fleshy and dry dehiscent fruits in *Cestrum* and *Brugmansia* (Solanaceae)

NATALÍ HERNÁNDEZ-CIRO and NATALIA PABÓN-MORA*

Instituto de Biología, Universidad de Antioquia, Medellín, Colombia

ABSTRACT The mechanisms controlling evolutionary shifts between dry and fleshy fruits in angiosperms are poorly understood. In Solanaceae, *Cestrum* and *Brugmansia* represent cases of convergent evolution of fleshy and dry fruits, respectively. Here we study the anatomical and genetic bases of the independent origin of fleshy fruits in *Cestrum* and the reversion to dry dehiscent fruits in *Brugmansia*.We also characterize the expression of candidate fruit development genes, including *ALCATRAZ/SPATULA, FRUITFULL, HECATE1/2/3, REPLUMLESS* and *SHATTERPROOF*. We identify anatomical changes to establish developmental stages in the ovary-to-fruit transition in *Cestrum nocturnum* and *Brugmansia suaveolens*. We generate reference transcriptomes for both species, isolate homologs for all genes in the fruit genetic regulatory network (GRN) and perform gene expression analyses for *ALC/SPT, FUL, HEC1/2/3, RPL* and *SHP* throughout fruit development. Finally, we compare our results to expression patterns found in typical capsules of *Nicotiana tabacum* and berries of *Solanum lycopersicum* available in public repositories. We have identified homologous, homoplasious and unique anatomical features in *C. nocturnum* and *B. suaveolens* fruits, resulting in their final appearance. Expression patterns suggest that *FUL*, *SHP* and *SPT* might control homologous characteristics, while *ALC* and *RPL* likely contribute to homoplasious anatomical features. The fruit GRN changes considerably in these genera when compared to typical capsules and berries of Solanaceae, particularly in *B. suaveolens,* where expression of *FUL2* and *RPL1* is lacking.

KEY WORDS: *ALCATRAZ, berry, capsule, FRUITFULL, fruit development, HECATE, REPLUMLESS*

Introduction

Fruits represent an extreme ontogenetic transformation in flowering plants. They result from the morpho-anatomical changes that the carpel wall suffers after the fertilization of ovules and during their transformation into seeds. Seed dispersal mechanisms have major ecological relevance in effective reproduction, population establishment and plant fitness (Bolmgren and Eriksson, 2005; Avino *et al*., 2012). Consequently, fruits exhibit an astonishing morphological diversity with remarkable different strategies ensuring seed nourishment and dispersal (Bobrov and Romanov, 2019).

Studies aimed to optimize fruit features using phylogenetic methods in many angiosperm families, have shown that fruit types are highly homoplasious (i.e. displaying similar morphologies as a result of convergent evolution and not from common ancestry). In general, fleshy fruits seem to have evolved several times independently from dry (often, dehiscent) fruits in different angiosperm lineages (Bolmgren and Eriksson, 2005). Here we focus on the Solanaceae, which contains major edible crops including eggplant, potato, pepper and tomato, as well as toxic species like jimsonweed and angel's trumpets. This family is ideal to assess the morpho-anatomical and genetic bases underlying fruit diversity for two main reasons. First, most species in this family possess a bicarpellate syncarpous gynoecium joined at the septum with axile placentation that produces either dry or fleshy fruits (Knapp, 2002; Pabón-Mora and Litt, 2011). Second, there have been relatively few changes in fruit evolution during the diversification of the family compared to other angiosperms. The documentation of fruit type occurrence onto the most recent Solanaceae phylogenetic

Abbreviations used in this paper: EDD, early divergent dry-fruited; GRN, genetic regulatory network; LDF, late divergent fleshy-fruited.

***Address correspondence to:** Natalia Pabón-Mora. Instituto de Biología, Universidad de Antioquia, Cl. 67 # 53-108, Medellín, Antioquia, Colombia. Tel: +57 1 3217720164. E-mail: lucia.pabon@udea.edu.co - web: https://www.evodevoplantas.com - https://orcid.org/0000-0003-3528-8078

Supplementary Material (11 figures and 2 tables) for this paper is available at: https://doi.org/10.1387/ijdb.200080np

Submitted: 14 February, 2020; *Accepted:* 5 April, 2020; *Published online:* 20 August, 2020.

ISSN: Online 1696-3547, Print 0214-6282

analysis suggests that dry fruits, both indehiscent and dehiscent are plesiomorphic, as they are characteristic of early-diverging lineages (including Goetzeoideae, Schwenckieae, Petunieae, Cestroideae and Nicotianoideae) and fleshy fruits were acquired in the late-diverging Solanoideae subfamily (Knapp, 2002) (Fig. 1). Nevertheless, there are some exceptions to this pattern. Fleshy fruits have evolved independently at least two times, in *Cestrum* L. (Cestroideae) and *Duboisia* R.Br (Nicotianoideae). Also, within Solanoideae there is at least one reversion to capsules, in the Datureae G.Don, that includes *Brugmansia* Pers.*,Datura* L. and *Trompettia* J.Dupin (Dupin and Smith, 2018). Most research so far has focused on identifying general anatomical features occurring during fruit development in different species. However, it is yet unclear what are the anatomical shifts and the genetic bases underlying the independent evolution of fleshy fruits and the reversion to dry fruits in the above-referred cases.

Arabidopsis thaliana (L.) Heynh has served as the most important reference species in the identification of the genetic regulatory network (GRN) that controls fruit development. *Arabidopsis* produces a silique, which is a special dry dehiscent fruit where the valves separate from the persistent medial tissue (i.e. the replum, unique to Brassicaceae) along the valve margin. Here, two layers form the dehiscence zone: the one closer to the valves becomes lignified, and the one, closer to the replum, persists as a non-lignified separation layer that disintegrates due to mechanical tension allowing dehiscence (Avino *et al.*, 2012; Ferrándiz, 2002). Six transcription factors control fruit patterning in *Arabidopsis*. *FRUITFULL (FUL),* a MADS-box transcription factor, *a*nd *REPLUMLESS (RPL),* a homeodomain protein, control valve and replum development, respectively (Gu *et al*., 1998; Roeder *et al*., 2003). Both *FUL* and *RPL* repress *SHATTERPROOF1/2 (SHP1/2)*, also MADS-box proteins, responsible for downstream activation of the bHLH genes *ALCATRAZ (ALC)* and *INDEHISCENT (IND).* While *ALC* forms the separation layer, *IND* controls the formation of the lignified layer (Heisler *et al.,* 2001; Girin *et al*., 2011; Kay *et al*., 2013; Liljegren *et al*., 2000; Liljegren *et al*., 2004). Finally, *SPATULA (SPT),* is redundant with its paralog *ALC* in the specification of the non-lignified layer of the dehiscence zone (Groszmann *et al*., 2011).

Gene homologs participating in the fruit GRN have been identified in several Solanaceae species, but most expression and functional data come from *Solanum lycopersicum* L. (with berries) and *Nicotiana benthamiana* Domin (with capsules) (Bemer *et al*., 2012; Burko *et al*., 2013; Fourquin and Ferrándiz, 2012; Garceau *et al*., 2017; Maheepala *et al*., 2019; Ortiz-Ramírez *et al*., 2018; Smykal *et al*., 2007). Altogether, the data gathered so far suggest a common GRN controlling dehiscence in dry fruits and ripening in fleshy fruits through the conserved FUL-SHP functional module in the first regulatory tier (Fourquin and Ferrándiz, 2012). As a result, the genetic switches allowing transformations between dry and fleshy fruits are more likely to occur in the downstream genes of the GRN including *RPL, ALC/SPT* and *IND.*

In Solanaceae, natural variation results in the independent evolution of fleshy fruits in *Cestrum* and the reversion to dry dehiscent fruits in *Brugmansia.* These lineages represent a unique opportunity to identify the anatomical shifts, as well as candidate genes that control the acquisition of fleshiness and dehiscence, independently. Here we present: (1) the anatomical changes associated to the independent acquisition of fleshy fruits in *Cestrum*

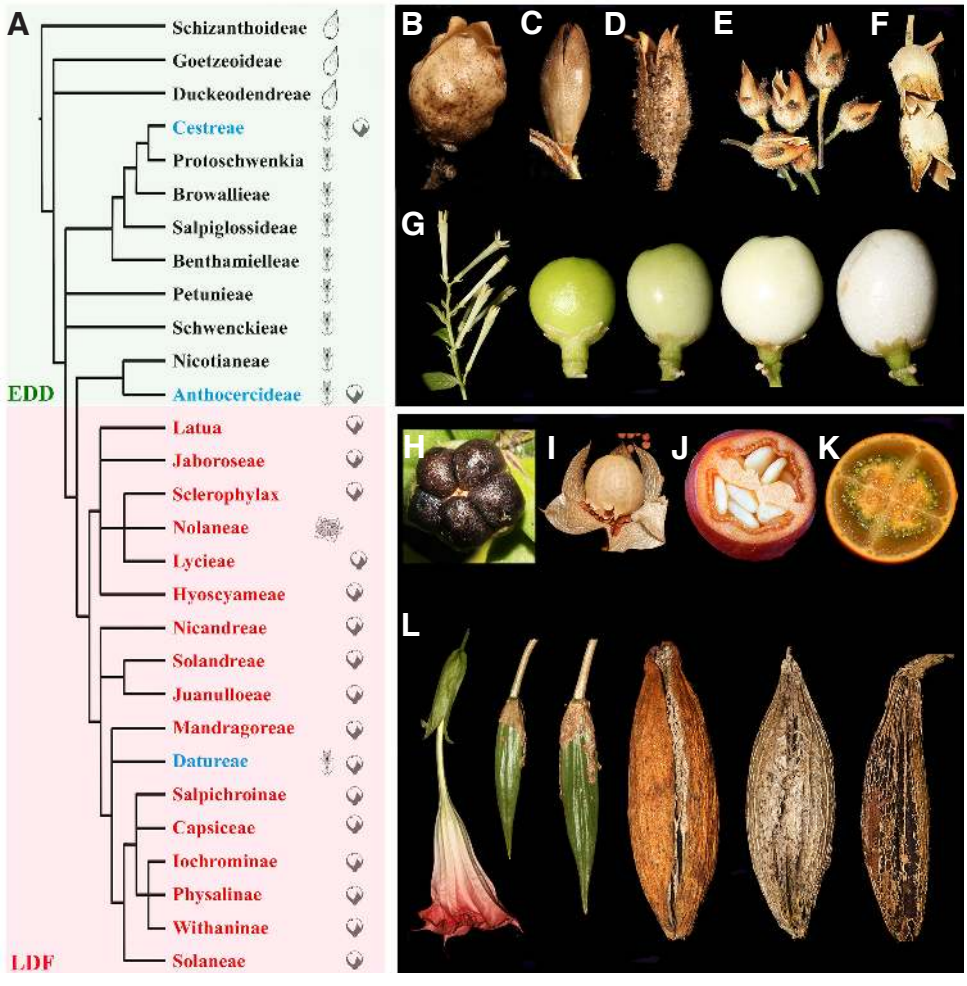

Fig. 1. Fruit diversity in the Solanaceae. (A) *fruit types optimized onto the phylogeny of the Solanaceae redrawn after Knapp* et al.*, 2002, showing the early divergent dry (EDD) fruited taxa and the late divergent fleshy (LDF) fruited taxa in green and red boxes, respectively. Drawings indicate drupes, dry deshicent fruits, fleshy fruits and mericarps in front of each lineage.* **(B-F)** *Representatives of the EDD lineages including* Schizanthus pinnatus *(B),* Nierembergia hyppomaniaca *(C),* Salpiglossis sinuata *(D),* Petunia hybrida *(E) and* Nicotiana sylvestris *(F).* **(G)** *Developmental series in the ovary-to-fruit transformation of the fleshy fruited* Cestrum nocturnum. **(H-K)** *Representatives of the LDF lineages including* Nolana humifusa *(H),* Nicandra physalodes *(I),* Capsicum annuum *(J), and* Solanum quitoense *(K).* **(L)** *Developmental series in the ovary-tofruit transformation of the dry fruited* Brugmansia suaveolens.

nocturnum L., as well as the reversion to dry dehiscent fruits in *Brugmansia suaveolens* (Humb. & Bonpl. ex Willd) Sweet; (2) the genetic complement in the fruit development GRN for the two species; and (3) expression patterns of all gene homologs found in the two species across different fruit developmental stages. Our results are discussed in the context of the previously reported anatomical features, genetic complement and gene expression for typical berries and capsules in Solanaceae.

Results

Anatomical changes during flower-to-fruit transition in Cestrum nocturnum

We followed the anatomical changes during preanthesis, anthesis and fruit development in *Cestrum nocturnum.* Our first stage sampled corresponds to the ovary in a 5 mm long floral bud, where the ovules have two integuments, and are curving towards an anatropous position. At this stage, the ovary wall is formed by eight cell rows of parenchymatic isodiametric cells (data not shown). When the floral bud reaches 10 mm, the ovary wall maintains eight cell rows of parenchymatic cells and some differentiation can be seen in the outer epidermis with rectangular cells and in the inner epidermis with smaller tangentially elongated cells (Fig. 2 B,C). At this stage, each carpel is supplied by one main vascular bundle. The cell nuclei are colored with safranin and the staining pattern indicates active cell division in the ovules and throughout the ovary wall (Fig. 2 B,C).

Anthesis occurs approximately when the grown corolla reaches 13 mm long (Fig. 2A). The number of cell layers in the ovary wall at this stage remains constant, however, tissue differentiation begins at this stage as lignification occurs in the form of sclereids, in the inner 2-3 layers of the fruit wall (i.e. the endocarp; Fig. 2D, E). The septum is formed by five rows of isodiametric parenchymatous cells. Each carpel is supplied by a main vascular bundle and 2 lateral smaller vascular traces (Fig. 2 D,E).

In a 2 mm (in diameter) fruit, hereafter called F1, there is evidence of both anticlinal and periclinal cell division, resulting in a slight increase in the total number of cell layers up to 10-13 (Fig. 2F). Increase in cell size in the mesocarp also contributes to fruit enlargement. The pericarp tissues have little variation when compared to F0, however at the fruit apex, lignification of the endocarp is almost continuous (Fig. 2F). The lignification of the endocarp reaches the mid-level of the fruit but not its base (Fig. 2G and data not shown). The cells of the exocarp remain small and tangentially elongated while cells of the mesocarp exhibit cellular expansion and are mostly spherical. At this stage the septum seems to be stretched and formed by three rows of flattened cells (Fig. 2G).

When the fruit reaches 5 mm, hereafter referred to as F2, cell expansion is predominantly responsible for the size increase, however, the number of cell layers reaches 14 by limited periclinal cell division (Fig. 2A). The clusters of lignified cells become scattered due to cell expansion in the parenchymatous cells in the pericarp (Fig. 2 H,I). Six vascular bundles irrigate each carpel.

In the 7 mm fruit, which corresponds to F3, periclinal division results in an increase in cell layers up to 15-16 (Fig. 2 A,J,K). At

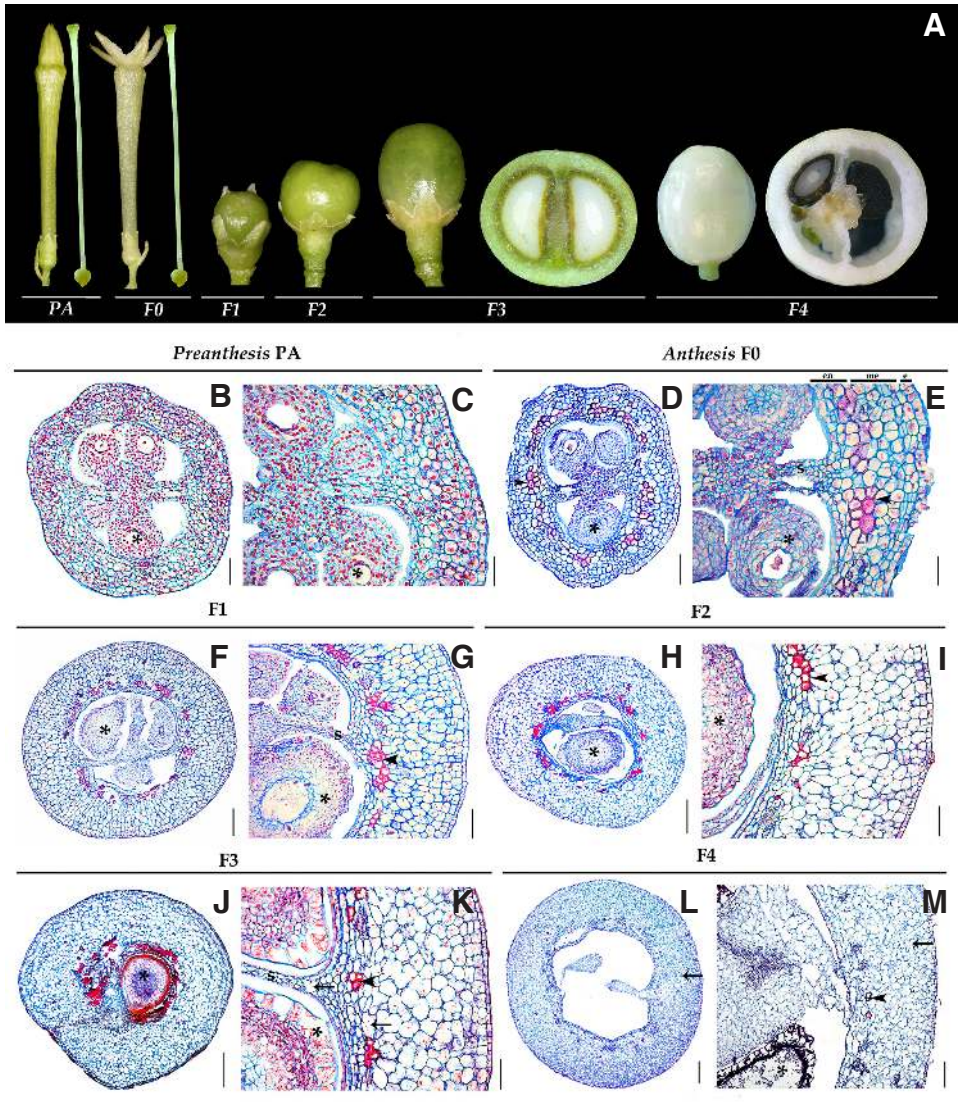

Fig. 2. Ovary-to-fruit morpho-anatomical changes in *Cestrum nocturnum*. (A) *Developmental series showing the ovary at preanthesis, anthesis and four different fruit developmental stages (F1 - F4).* **(B-E)** *Ovary wall at preanthesis* **(B,C)** *in a 10 mm floral bud and anthesis* **(D,E)** *in a 13mm floral bud.* **(F-M)** *Cross sections of the pericarp when the fruit reaches 2 mm* **(F,G)**, *5 mm* **(H,I)**, *7 mm* **(J,K)** *and 10mm* **(L,M)** *of diameter. e, exocarp; en, endocarp; me, mesocarp; s, septum. Asterisks indicate ovules and seeds; arrowheads point to lignification; arrows indicate lacunae. Scale bars: 50 um in C, E, H, J, and L; 100 um in D, I, K and G; 200 um in B, F and M.*

the apical portion, the lignification of the endocarp is still evident with cells now entering complete cytoplasm degradation and cell death (Fig. 2J). At the mid-level of the fruit, lignification is now less conspicuous as only few clusters of sclerenchymatic cells remain unevenly distributed (Fig. 2K). The septum is formed by three rows of parenchymatous cells and lacunae are formed (Fig. 2K). At this stage, a thin cuticle develops over the exocarp (Fig. 2K). The number of vascular traces remains constant.

In the 10 mm fruit, hereafter referred to as F4, a considerable increase in thickness of the pericarp and fruit size is observed (Fig. 2A). In *C. nocturnum*, fruit maturation is accompanied by the softening of the pericarp and a change from green to white (Fig 2A). The number of cell layers has increased to 19-21 through periclinal cell division (Fig. 2 L,M). However, anticlinal cell division and cell expansion, also contribute to the increase in fruit size. Lignification continues at the apex and at the mid-level of the fruit, accompanied with abundant lacunae (Fig. 2M). Unlike in the previous stages, the cells of the endocarp as well as those of the septum begin to soften and degrade (Fig. 2M). At this stage, the placenta proliferates and expands toward the pericarp to surround the seeds (Fig. 2M).

Anatomical changes during flower-to-fruit transition in Brugmansia suaveolens

Contrary to *C. nocturnum*, it is hard to find *B. suaveolens* setting fruits in the field. This is likely due to selfincompatibility as abundant flowers are seen. Thus, a one to one comparison for all developmental stages with *C. nocturnum* could not be done. Here we describe the stages as comprehensively as possible based on our collections (Fig. 3A).

The ovary of *B. suaveolens* in the 7 cm pre-anthethic (PA) floral bud has ca. 30 cell layers and is composed of parenchymatous tissue (Fig. 3B,C). The vascular bundles serve as a limit between smaller cells to the outside until the outer epidermis and bigger cells to the inside (Fig. 3B,C). The inner and outer epidermis are formed by small rectangular cells. Each carpel is supplied by one main vascular bundle and ca. 15 lateral smaller traces. The flowers enter anthesis when the corolla reaches 24-32 cm (Fig. 3A). The ovary wall after anthesis, hereafter called F0, is anatomically similar to preanthesis. The number of cell layers and vascular traces remains constant. Main differences are seen in the exocarp, which develops a thick cuticle and the size increase in the mesocarp cells (i.e. those outside of the vascular bundles) (Fig. 3 D,E).

According to our sampling, F1 corresponds to a dark green 10 cm long fruit (Fig. 3A). At this point there has been a considerable increase in fruit size primarily as the result of extensive anticlinal and periclinal cell division. The number of pericarp layers is ca. 50 (Fig. 3F,G). The endocarp and mesocarp are readily differentiated due to distinct cell size, shape and orientation. In the endocarp, primarily tangentially elongated small cells are present, while in the mesocarp spherical, larger cells are the norm (Fig. 3 F,G). The septum thickens as a result of anticlinal and periclinal division (Fig. 3G). The size of the vascular traces is notably larger in comparison to previous stages.

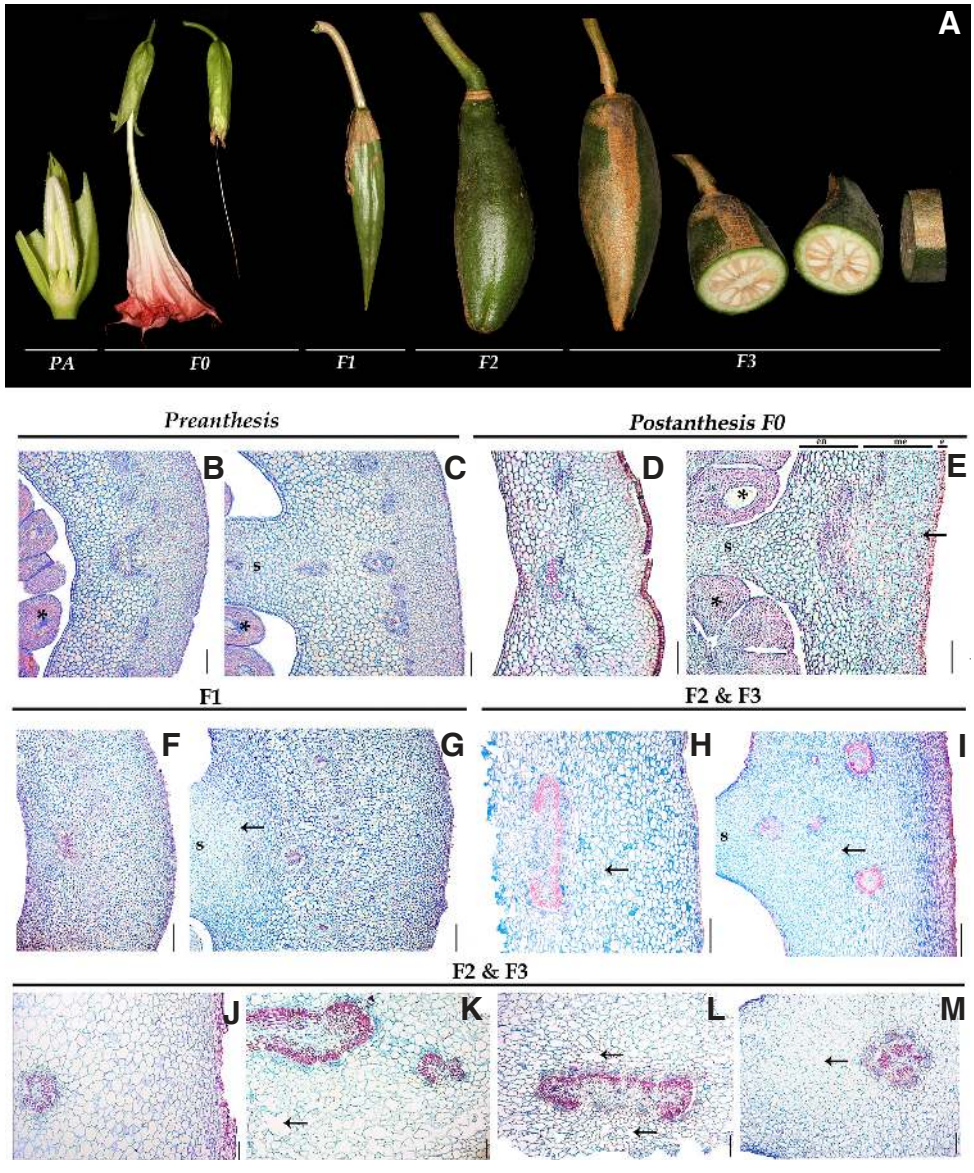

Fig. 3. Ovary-to-fruit morpho-anatomical changes in *Brugmansia suaveolens*. (A) *Developmental series showing the ovary in preanthesis, anthesis and three different fruit developmental stages (F1-F3).* **(B-E)** *Ovary wall at preanthesis in a 7 cm floral bud* **(B-C)** *and anthesis* **(D,E)** *in a 26 cm long flower.* **(F-I)** *Cross sections of the pericarp when the fruit reaches 10 cm* **(F,G)**, *and 20 cm* **(H,I)**. **(J-M)** *Detail of the exocarp and endocarp at F3 (J), the vascular traces at septum* **(K,M)** *and the mid vein* **(L)**. *e, exocarp; en, endocarp; me, mesocarp; s, septum. Asterisks indicate ovules and seeds; arrowheads point to lignification; arrows indicate lacunae. Scale bars: 100 um in D, E and; 200 um in B, C, M, L; 500 um in F, G, J, K, H and I.*

The following stages, described as F2 and F3, correspond to when the fruit has achieved ca. 20 cm long. The fruit appearance is still dark green, but the number of cell layers has increased to ca. 60 (Fig. 3 H,I). The exocarp cells remain squared and small. The mesocarp cells are irregular but remain tightly packed, while in the endocarp there are abundant intercellular spaces. One of the most remarkable changes at this stage is the increase in size of the vascular bundles in comparison to F1 (Figs. 3 H,I). Moreover, vascular tissue organization differs between the traces in the septum and the mid-vein. The septum vascular bundles are collateral open and seem to be organized in poles. In contrast, the mid-vein has a horseshoe shape (Fig. 3H). At the mid-vein, detachment between endocarp cells results in intercellular spaces, as if the vascular bundle produced tension (Fig. 3H). Peripheral pericarp vascular bundles form a semi-continuous ring of xylem and are surrounded by abundant lacunae, also supporting the idea that bundles are actively generating tension in the pericarp (Fig. 3I).

During maturation, the fruit does not soften. Although the pericarp thickness increases, we do not observe the presence of collenchyma or any other support tissue. Fruits stop growing when they reach ca. 20 cm long and the exocarp gradually shifts from dark green to brown (Figs. 1,3A). This change occurs irregularly throughout the pericarp, due to drying accompanied by cell death. Interestingly, this is observed at the cellular level, as the exocarp and the outer mesocarp layers develop secondary cell walls (Fig. 3J). During final stages of maturation cell death occurs more regularly in the pericarp, except in the vascular bundles allowing seed dispersal (Figs. 1,3A).

Evolution and expression of genes controlling fruit development

*T*o investigate the genetic mechanisms controlling fruit development in *C. nocturnum* and *B. suaveolens* we isolated gene homologs from the fruit GRN and assessed their expression in different developmental stages. We present our results gene by gene.

The FRUITFULL genes

As most Solanaceae species, *C. nocturnum* and *B. suaveolens* have three to four copies of *FUL-like* genes (Maheepala *et al*., 2019). *Brugmansia suaveolens* has orthologs of *FUL1*, *FUL2*, *MBP20* and *MBP10.* Similarly, *C. nocturnum* has homologs for all clades, except for *MBP10* (Supplementary Fig. S1).

FUL genes are broadly expressed throughout fruit development in both *C. nocturnum* and *B. suaveolens*. The *euFULI* orthologs in *C. nocturnum*, *CenoFUL1* and *CenoFUL2* are expressed in all developmental stages tested in the carpel-to-fruit transition with very low expression in F4 (Fig. 4). The expression of *euFULI* genes in *B. suaveolens* is very different, as *BrsuFUL1* is expressed in all stages except F1 and F2, while *BrsuFUL2* is not detected in carpels or fruits at any developmental stage. The only *euFULII* ortholog from *C. nocturnum*, *CenoMBP20,* is strongly expressed in F0 and F1, then the expression is reduced at F2 and it has a subtle increase at F3. The *euFULII* homologs, *BrsuMBP20* and *BrsuMBP10* have similar expression patterns, with strong expression at early stages of fruit development and then a reduction at F1 and F2 with a subsequent increase at F3 (Fig. 4).

The AGAMOUS/SHATTERPROOF genes

As other Solanaceae species, *C. nocturnum* and *B. suaveolens* have one copy of *AGAMOUS* (Ortiz-Ramírez *et al*., 2018).

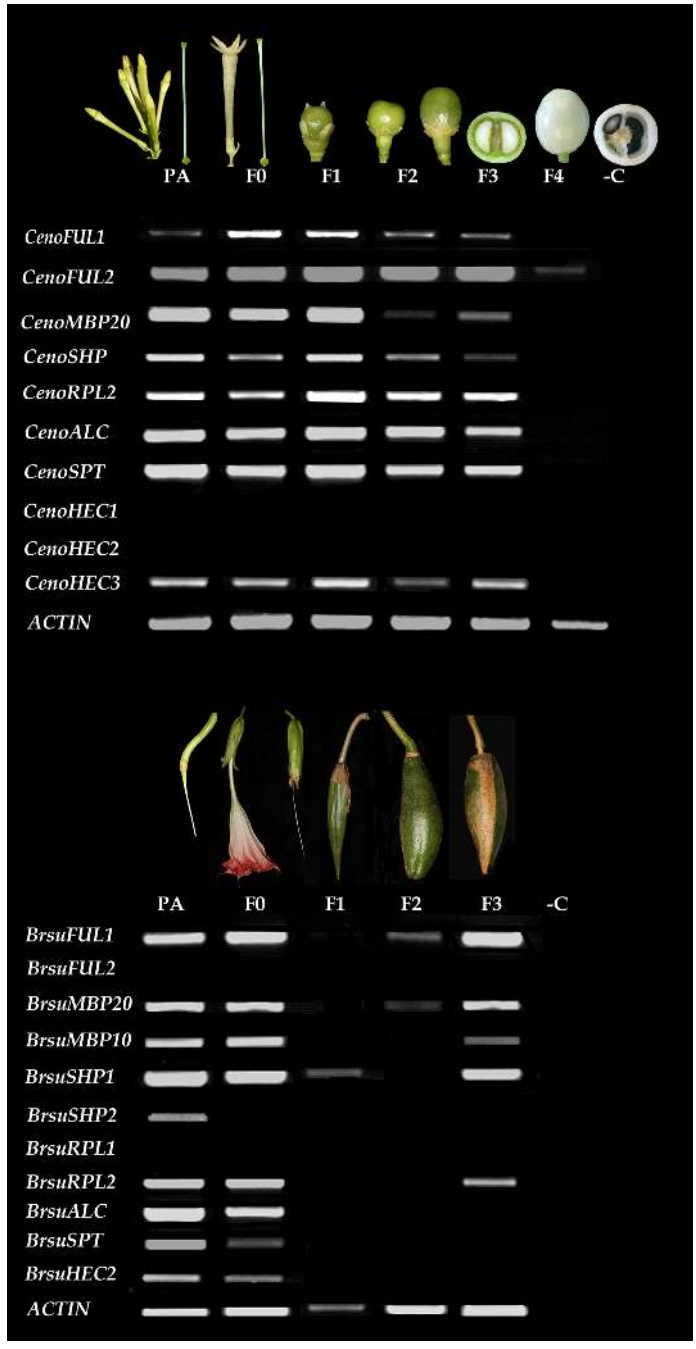

Fig. 4. Expression analyses of the fruit genetic regulatory network (GRN) genes in *Cestrum nocturnum* and *Brugmansia suaveolens*. *PA, ovary in preanthesis; F, fruit developmental stages; Actin was used as a positive control; -C indicates the amplification reaction loaded without cDNA.*

On the other hand, while *C. nocturnum* has one *SHP* copy, in *B. suaveolens* we identify two *SHP* variants (i.e. *BrsuSHP1* and *BrsuSHP2*). *BrsuSHP2* is *8*0bp longer in its CDS than *BrsuSHP1* (Supplementary Fig. S2).

As *AG* homologs are related with stamen and carpel identity and *SHP* genes have been shown to play roles in fruit development, only expression of the latter was tested in RT-PCR. *SHP* genes present different expression patterns in the two species. *CenoSHP*

expression is constant across carpel-to-fruit development with a subtle decrease after F2. In contrast, *BrsuSHP1* expression is strong at PA and F0, it decreases at F1 and F2 but comes up again during F3. Finally, *BrsuSHP2* expression was detected exclusively at PA (Fig. 4).

The REPLUMLESS genes

Most Solanaceae species have two copies of *RPL* (Ortiz-Ramírez *et al*., 2018). We find these two copies in *B. suaveolens* (B*rsuRPL1 and BrsuRPL2*), and only one copy, the *RPL2* ortholog, in *C. nocturnum* (Supplementary Fig. S3).

RPL expression patterns also differ between *C. nocturnum* and *B. suaveolens*. *CenoRPL2* expression is homogeneous throughout fruit development with a stronger expression at F1. Conversely, *BrsuRPL1* expression is not detected at any developmental stage while *BrsuRPL2* expression is restricted to PA, F0 and later on F3.

The SPATULA/ALCATRAZ genes

As in other Solanaceae species, one copy of *SPT* and one copy of *ALC* are present in *C. nocturnum* and *B. suaveolens* (Supplementary Fig. S4).

SPT/ALC genes exhibit opposite expression patterns in *C. nocturnum* compared to *B. suaveolens*. While *CenoSPT and CenoALC* are expressed homogeneously across all stages of carpel-to-fruit development, the expression of *BrsuSPT* and *BrsuALC* is restricted to the carpel in preanthesis and F0 (Fig. 4).

The HECATE1/2/3 genes

Most Solanaceae species have two copies of *HEC1* and *HEC2* and single copies of *HEC3* (Ortiz-Ramírez *et al*., 2018). For *C. nocturnum* we detect single copies for *HEC1/2/3* (i.e. *CenoHEC1*, *CenoHEC2* and *CenoHEC3*). In contrast, a single *HEC2* ortholog *w*as isolated from the *B. suaveolens* transcriptomes and no matches were found for *HEC1* or *HEC3* homologs (Supplementary Fig. S5).

CenoHEC1 and *CenoHEC2* are not detected after 30 amplification cycles, and only *CenoHEC1* is detected at F1, after 35 amplification cycles (Supplementary Fig. S6). *CenoHEC3* has similar broad (but low) expression patterns across carpel-to-fruit

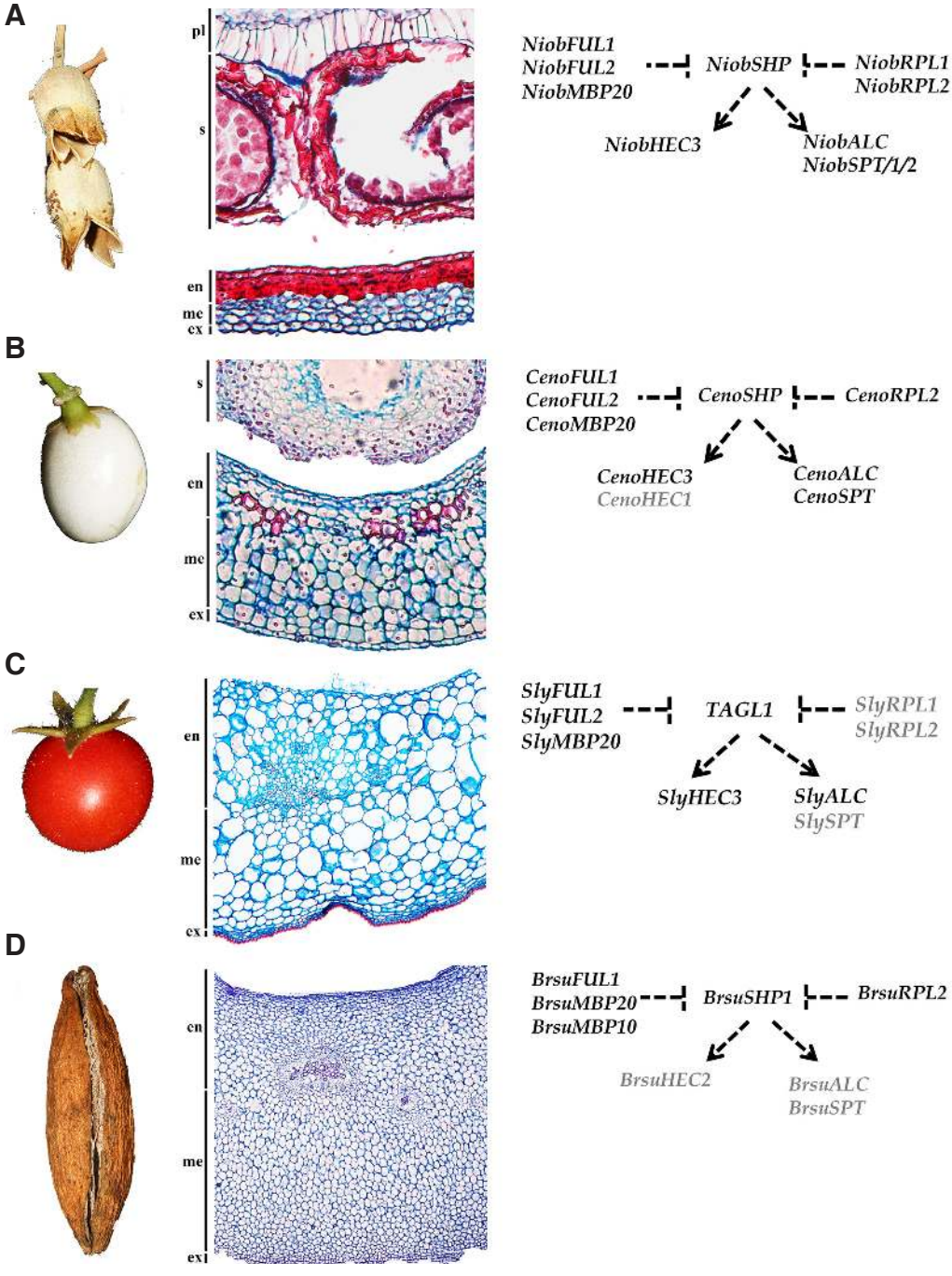

Fig. 5. Summary of fruit anatomical features and the genetic complement of the fruit genetic regulatory network (GRN) in representative Solanaceae. *Fruit pictures, cross section of the fruit and the fruit GRN are shown for selected taxa.* **(A)** Nicotiana obtusifolia, *as a representative of the typical capsule.* **(B)** Cestrum nocturnum, *with a homoplasious fleshy fruit.* **(C)** Solanum lycopersicum, *as a representative of the typical berry.* **(D)** Brugmansia suaveolens, *with an independently acquired dry fruit. en, endocarp; ex, exocarp; me, mesocarp; pl, placenta; s, seed; gray letters indicate that gene expression is restricted to early stages of fruit development. Dotted lines indicate that these putative interactions based on the model* Arabidopsis thaliana *have not been confirmed in Solanaceae.*

development except at F2 where expression decreases. *BrsuHEC2* is *d*etected only at PA and F0 (Fig. 4).

Discussion

The homologous, the homoplasious and the unique anatomical features in C. nocturnum and B. suaveolens fruits

Here we identify homologous anatomical features (i.e. that correspond with their phylogenetic position) shared between *C. nocturnum* and closely related taxa with capsular fruits, as well as between *B. suaveolens* and closely related taxa with fleshy fruits. We also describe homoplasious features, which result in the final fruit appearance. Finally, we list those unique anatomical combinations occurring in the two convergent fruit types (Fig. 5). In general, we find that ovary wall anatomical features in preanthesis cannot predict fruit type and it is the combination of developmental shifts, and changes in gene expression, what results in convergent evolution of fruit types in the Solanaceae.

Our data as well as that previously generated by Pabón-Mora and Litt (2011) points to a series of anatomical features that can distinguish different early and late diverging fruit types in Solanaceae. Common features present in early divergent dry-fruited (EDD) and dehiscent taxa include: (1) a constant (or a limited increase) number of cells in the ovary wall and pericarp; (2) basipetal and centripetal lignification in the endocarp; (3) discontinuous lignification in the septum; (4) elongation prior to the drying of the placenta epidermal cells; and (5) dehiscence. Conversely, common features in late diverging fleshy-fruited (LDF) taxa, include: (1) an increase in the number of layers during carpel-to-fruit transition and throughout fruit development; (2) cell expansion in the pericarp; (3) formation of collenchyma in the mesocarp; (4) expansion of the endocarp into the locules; and (5) ripening, accompanied with plasticity in the mature fruit size (Fig. 5).

From these features, *C. nocturnum* shares with the EED taxa, the limited increase in the number of cell layers in the ovary-to-fruit wall, and the basipetal, centripetal and discontinuous endocarp lignification (Figs. 1,2). These homologous features occur early in development similar to what has been detected in other species of *Cestrum*, like *Cestrum diurnum* L. (Pabón-Mora and Litt, 2011). Homoplasious features resulting in the apparent fleshy fruits of *C. nocturnum* include cell expansion in the pericarp cells and ripening, both occurring late in development, also like in *C. diurnum* (Pabón-Mora and Litt, 2011). The placenta remains fleshy in accordance to the seed dispersal strategy by endozoochory (Cortés-Flores *et al*., 2013). The simultaneous presence of a discontinuous lignified endocarp and a mesocarp undergoing cell expansion lacking collenchyma is unique to *Cestrum* within early divergent Solanaceae taxa.

In comparison, *B. suaveolens* shares with the LDF taxa *t*he considerable increase in fruit size due to anticlinal and periclinal cell division, and cell expansion, as well as the absence of lignification in the pericarp. This contrasts with the closely related species *Datura inoxia* Mill. that produces dry dehiscent fruits, where lignification in form of fibers occurs in the mesocarp (Pabón-Mora and Litt, 2011). Periclinal and anticlinal cell division and cell expansion begin early in the ovary-to-fruit transition. Conversely, homoplasious features include the formation of lacunae, especially surrounding the vascular traces. Intercellular spaces are common among EED taxa but are rare in LDF taxa (Pabón-Mora and Litt, 2011).

Unique late developmental features observed in *B. suaveolens* include: (1) pericarp degradation in between the vascular tissue, (2) lacunae around the vascular tissue and (3) changes in cell orientation and size between the endocarp and the mesocarp, all consistent with pericarp withering and seed release by mechanical means as a dispersal strategy (Fig. 1). However, we cannot rule out seed dispersal by animals before pericarp withering. Such differences between endocarp and mesocarp are reminiscent of late fruit development in *Datura inoxia*, where cell division continues in mesocarp but stops in the endocarp and appears to result in the formation of lacunae (Pabón-Mora and Litt, 2011). Accordingly, many diagnostic characteristics of LDF taxa are lacking in *B. suaveolens* including the presence of collenchyma at the mesocarp and the fleshy, placenta or endocarp proliferation into the locules (Pabón-Mora and Litt, 2011). Tissue degradation is common in the inflated calyx protecting the *Physalis* berries and in *Alkekengi officinarum* Moench (Solanoideae) (Supplementary Fig. S7; Owen, 1840). This suggests such process is not unique to *B. suaveolens* fruits but it also occurs in other Solanoideae, although not necessarily in fruits.

In order to hypothesize which genes are likely responsible for the homologous and the homoplasic features in *C. nocturnum* and *B. suaveolens* fruits, we compared *ALC/SPT*, *FUL,* H*EC1/HEC2/HEC3*, *RPL* and *SHP* expression patterns in the ovary-to-fruit transition of the two species (Fig. 5). We analyzed these results in comparison to the expression reported or identified for *Nicotiana benthamiana*, as a representative of the EDD taxa, and *Solanum lycopersicum*, as a representative for the LDF taxa (Fig 5). Nonetheless, all comparisons and conclusions reached based on comparative anatomy and expression data will require functional assessments in the future.

FRUITFULL genes have similar broad expression patterns in both C. nocturnum and B. suaveolens fruits

Three *FUL* genes (*FUL1, FUL2* and *MBP20*) were isolated in *C. nocturnum,* which is consistent with previous studies pointing to a late *MBP10/MBP20* duplication event in the *euFULII* clade occurring only after the diversification of the Petunieae (Maheepala *et al*., 2019). The three copies are expressed throughout ovary-to-fruit development. However, the *euFULI* genes (i.e. *CenoFUL1* and *CenoFUL2*) have a constant expression until fruit maturity while *CenoMBP20* lowers its expression dramatically after F1. Our results suggest that in *C. nocturnum*, all *FUL* genes are important in the early developmental stages, but only *euFULI* genes are active in late stages of fruit development. Results for *B. suaveolens* are strikingly different. First, a complete set of four *FUL-like* genes was isolated. *S*econd, their expression, although broad, has two peaks, the first one at and right after anthesis, and the second one at late stages of fruit development at F3. Third, an exception occurs with *BrsuFUL2*, which remained undetected throughout the stages sampled. When our data is compared to the expression and functions reported for *FUL-like* genes in *S. lycopersicum* and *N. tabacum* (Supplementary Fig. S8), we see that *euFULI* genes are likely performing the most important roles in late fruit development when compared to *euFULII* genes (Bemer *et al*., 2012). In this context, the lack of expression of *BrsuFUL2* represents a major difference in the GRN and broader comparative studies are required to test the impact of this change in fruit morphology.

SHATTERPROOF and REPLUMLESS genes have different expression patterns in C. nocturnum and B. suaveolens fruits

Together with *FUL*, *SHP* and *RPL* homologs are major players in the early histogenesis of fruits (Ferrándiz *et al*., 2000; Vrebalov *et al*., 2009). In fact, *SHP* and *RPL* show fluctuating expression patterns in different species and fruit types (Supplementary Fig. S9). The *SHP* homologs isolated, show different expression patterns in the two species studied. *CenoSHP* is present from preanthesis to late stages in fruit development, with a peak at F1. Conversely, the two paralogs from *B. suaveolens* have redundant expression only in the preanthethic carpel, afterwards their expression differs dramatically, as *BrsuSHP1* is continuously detected during fruit development (except at F2), but *BrsuSHP2* is turned off (Fig. 4). The high expression of *SHP* homologs early during fruit development correlates with the increase of the number of pericarp cell layers in both *C. nocturnum* and *B. suaveolens.* This latter role was also reported in tomato, where *TAGL1* regulates pericarp thickness (Vrebalov *et al*., 2009). However, a role of *CenoSHP* in the early fruit patterning through the control of lignified *vs* unlignified layers upstream *ALC* and *HEC*, cannot be ruled out. This is hypothesized based on the roles of *SHP* in dehiscence zone patterning reported for dry dehiscent fruits in Fabaceae, Solanaceae and Brassicaceae among others (Fourquin *et al*., 2013).

On the other hand, *RPL* functional analyses are scarce, but some *RPL* homologs have been recruited in different roles during fruit patterning and seed dispersal. *RPL* in *Arabidopsis* represses *SHP* and in turn helps provide independent identity to the medial persistent tissue called the replum (Roeder *et al*., 2003). *RPL* orthologs in rice control fruit shedding by the formation of an abscission layer between the pedicel and the fruit (Konishi *et al*., 2006). In addition, *RPL* homologs are turned on specifically in the dehiscence zone of dry dehiscent poppy fruits (Zumajo-Cardona *et al*., 2018). In Solanaceae functional analyses are lacking, but *RPL* expression is remarkably different between fleshy and dry fruits, as in dry dehiscent fruits *RPL* expression remains constant during the entire ovary-to-fruit transition, while it is reduced during ripening of the fleshy fruits (Ortiz-Ramírez *et al*., 2018).

The fact that *CenoRPL2* replicates the typical expression of *RPL* homologs in dry fruits suggest that *RPL* is controlling homologous features present in *Cestrum* and the EED taxa. These include limiting periclinal cell division, promoting lignification, restricting cell expansion and retaining a fully parenchymatous septum. On the other hand, in *B. suaveolens*, the two *RPL* homologs have different expression patterns. While *BrsuRPL1* is not expressed in any of the developmental stages studied here, *BrsuRPL2* is first active in preanthesis and in F0, then turned off during development, and finally turned on again at F3 (Fig. 4). The loss of *BrsuRPL1* activity may imply important changes in fruit patterning. Conversely, *BrsuRPL2* expression replicates the typical expression of *RPL* homologs in fleshy fruits early on, suggesting that here also *RPL* is controlling homologous features shared between *B. suaveolens* and the LDF taxa early in development. These include the negative control of cell expansion early on and the retention of parenchymatous tissue in the septum (medial tissue). These are features attributed to *RPL* genes in other angiosperms. Moreover, the reduced *RPL* expression late in development shared by *B. suaveolens* and the LDF taxa correlate well with the onset of cell expansion.

SPATULA expression coincides with the occurrence of homologous anatomical features while ALCATRAZ expression correlates with homoplasious fruit features

The remaining genes from the fruit GRN differ drastically in their expression between the two target species. Previous studies have found opposite expression patterns of *SPT/ALC* in capsules and berries of Solanaceae, providing a reference for other fruit types in this family. While the expression of *SPT* is maintained throughout the development of dry dehiscent fruits, *ALC* is turned off in late stages of development. Conversely, *SPT* is turned off late in fleshy fruit development and *ALC* expression is maintained (Ortiz-Ramírez *et al*., 2018).

Comparatively, in *C. nocturnum SPT* expression in all stages of fruit development coincides with that observed in capsules of *Brunfelsia australis* Benth. other closely related EED taxa. Conversely, the maintained expression of *ALC* matches with the pattern observed in berries of *Capsicum annuum* L. and *S. lycopersicum* (Fig. 4, (Ortiz-Ramírez *et al*., 2018). In *B. suaveolens, SPT* expression coincides with that shown by closely related LDF taxa inside the Solanoideae as it is turned off in later stages of fruit development. In contrast, *ALC* expression resembles that of the capsules of *B. australis* (Fig. 4; Ortiz-Ramírez *et al*., 2018).

SPT/ALC function in Solanaceae has been evaluated using virus induced gene silencing (VIGS) in *N. obtusifolia* with capsules, and *C. annuum* and *S. lycopersicum* with berries. Single gene downregulated plants did not show abnormal fruit phenotypes compared to the wild type plants. However, when both *SPT* and *ALC* were downregulated lignification occurs earlier and ectopically in both fruit types, suggesting that the two genes redundantly repress lignification (Ortiz-Ramírez *et al*., 2019). This is consistent with the role of *ALC* in the *Arabidopsis* fruit, where it enables cell separation and dehiscence by promoting the differentiation of the non-lignified cells in the dehiscence zone (Rajani and Sundaresan, 2001). *ALC* is likely playing a direct or indirect role in preventing lignification in the separation layer (Rajani and Sundaresan, 2001; Roeder and Yanofsky, 2006). Thus, *ALC* might be a good candidate gene for explaining the homoplasic features observed in *C. nocturnum* and *B. suaveolens* fruits. In *C. nocturnum* and berries of Solanaceae, *ALC* might control extreme cellular expansion late in fruit development and might prevent lignification across the pericarp. In contrast, in *B. suaveolens* and capsules of Solanaceae*, ALC* downregulation could be related to the emergence of lacunae in the pericarp.

Only HECATE3 genes seem to have a role in fruit development in C. nocturnum

Among all genes isolated, the *HEC/IND* homologs were the most variable in terms of copy number isolated from the two target species. Whereas *HEC1/2/3* homologs were isolated from *C. nocturnum*, only one *HEC2* ortholog was identified in *B. suaveolens.* Their expression is also drastically different. While *CenoHEC3* is broadly expressed in all the ovary-to-fruit developmental stages sampled, *BrsuHEC2* is only active in the preanthethic gynoecium and in F0 (Fig. 4).

In *A. thaliana* the paralog of *HEC3, INDEHISCENT* is primarily responsible for controlling the lignification of margin cells during fruit dehiscence (Liljegren *et al*., 2004). *HEC1, 2* and *3* play an important role in carpel development by controlling proper post-genital fusion of the septum and the apical gynoecium as well as stigma and transmitting tract development (Gremski *et al*., 2007). Our data

point to functions of *CenoHEC3* in carpel and fruit development in *C. nocturnum*, similar to what was reported for other Solanaceae species (Ortiz-Ramírez *et al.*, 2018). On the other hand, *BrsuHEC2* is likely to have limited roles early in gynoecium patterning, more similar to what is observed in *Arabidopsis* (Gremski *et al.*, 2007).

In *Arabidopsis* all three *HEC* proteins interact and share functions with *SPT* (Gremski *et al.*, 2007; Schuster *et al.*, 2015). In the two species studied here and in other Solanaceae, expression of *HEC* and *SPT* coincides, suggesting that this interaction might be conserved in the family (Ortiz-Ramírez *et al.*, 2018). Consequently, *HEC3* might share functions with *SPT* in Solanaceae fruits, including the control of lignification.

Conclusion

Cestrum and *Brugmansia* fruits present unique anatomical features resulting from a combination between EED and LDF taxa characteristics (Fig. 5). Analysis of our expression data in light of previous studies suggests that *ALC* and *RPL* likely contribute to the homoplasious anatomical features in these species. Conversely, *FUL* genes, *SHP* S*PT* might control homologous characteristics. Furthermore, fruit GRN in *Cestrum* and *Brugmansia* considerably differs from *Arabidopsis* and typical capsules and berries of Solanaceae (Fig. 5). In *Cestrum HEC3* expression suggest a function not only in carpel but also in fruit development. In *Brugmansia* the lack of expression of *FUL2* differs radically from the classic GRN and its implications in fruit development should be examined. In both species, *euFULII* genes *MBP10* and *MBP20* expression suggest a role in carpel and fruit development not previously reported. Finally, these hypotheses should be tested through *In situ* hybridization and functional studies to identify the role of these genes in specific anatomical and morphological changes.

Materials and Methods

Anatomy of fruits and selection of developmental stages for gene expression analyses

Flowers and fruits of *Brugmansia suaveolens* and *Cestrum nocturnum* at different developmental stages were gathered from living collections at the Jardin Botánico de Medellín (vouchers Pabón-Mora N & Hernandez-Ciro N., 410, 411). Available plant material was fixed in 70% ethanol. For light microscopy, fixed material was manually dehydrated through an alcohol–histochoice series and embedded in Paraplast X-tra (Fisher Healthcare, Houston, TX, USA). The samples were sectioned at 10–20 μm with a Leica RM2125 RTS (USA) rotary microtome. Sections were stained with Johansen's safranin, to identify lignification and presence of cuticle, and 0.5 % Astra Blue and mounted in Permount (Fisher Scientific, Pittsburgh, PA, USA). Sections were viewed and digitally photographed with a Zeiss Axioplan compound microscope and a Zeiss stereoscope equipped with an AxioCamERc5s digital camera with ZEN software. Several stages based on size differences in the transition from carpel to fruit were selected for each species in order to identify the anatomical changes that occur during fruit development. For *C. nocturnum*, six developmental stages where selected. Measurements of floral buds and flowers were made from the base of the sepals to the tip of the elongating corolla. Preanthesis (PA) corresponds to the carpel in a 13 mm long floral bud; Fruit S0 (F0) corresponds to an 13 mm long anthethic flower; and Fruit S1-S4 (F1-F4) correspond to different fruit developmental stages at 2 mm, 5 mm, 7 mm and 10 mm of diameter, respectively (Fig. 2A). For *B. suaveolens*, four developmental stages were selected. Preanthesis (PA) corresponds to the carpel in a 7 cm long floral bud; Fruit S0 (F0) corresponds in this case to the fruit wall from a postanthethic flower with withering corolla; Fruit S1 (F1) corresponds to a 10 cm long fruit; and Fruit S2-S3 (F2-F3) correspond to a 15 cm long fruit, prior to drying. Descriptions of endocarp, mesocarp and exocarp were done in reference to the position of vascular bundles, following (Pabón-Mora and Litt, 2011).

RNA-seq and candidate gene identification

Reference transcriptomes were generated for *C. nocturnum* and *B. suaveolens* from mixed tissues including vegetative and reproductive meristems, floral buds, leaves and fruits at different developmental stages. The material was collected from the same specimens (vouchers referenced above) and flash frozen in liquid nitrogen. Plant material was ground using liquid nitrogen and total RNA extraction was carried out using TRizol Reagent (Invitrogen, USA). RNA-seq experiments for each species were conducted using a TruSeq mRNA library construction kit (Illumina) (one library per species) and sequenced in a HiSeq2000 instrument reading 100 bases paired-end reads. The transcriptomes were assembled *de novo* at the Centro Nacional de Secuenciación Genómica (CNSG). Read cleaning was performed with PRINSEQ-LITE with a quality threshold of Q35 and contig assembly was computed using the Trinity package, following default settings. For *C. nocturnum*, contig metrics are as follows: total assembled bases, 121964260 bp; total number of contigs, 142 459; average contig length, 856 bp; largest contig, 11926 bp; contig N50, 1340 bp; contig GC, 41.13 %. For *B. suaveolens*, contig metrics are as follows: total assembled bases, 109351485 bp; total number of contigs, 94 825; average contig length, 1153 bp; largest contig, 15820 bp; contig N50, 1851 bp; contig GC, 40.57 %.

Gene isolation and phylogenetic analyses

The homologs of *AGAMOUS/SHATTERPROOF, ALCATRAZ/SPATULA,* H*ECATE1/HEC2/HEC3/INDEHISCENT* and *REPLUMLESS* in Solanaceae species have been already identified by Ortiz-Ramirez *et al.,* (2018) using the *Arabidopsis Thaliana* sequences as a query. Additionally, the homologues of *FRUITFULL/APETALA1* have been previously isolated by Maheepala *et al.,* (2019). We compiled the genes previously isolated in these studies as a reference for our own BLAST hits from *C. nocturnum* and *B. suaveolens*. These sequences can be found under Genbank numbers MT069970- MT069993.

All sequences isolated were compiled using Aliview (Larsson, 2014) and manually edited to exclusively keep the ORF for all transcripts. Nucleotide sequences isolated from *C. nocturnum* and *B. suaveolens* were subsequently aligned to the previously aligned matrices from Ortiz-Ramírez *et al.,* (2018) and Maheepala *et al.,* (2019) implementing the option --add on the online version of MAFFT (https://mafft.cbrc.jp/alignment/software/) (Katoh, 2002) with a gap open penalty of 4.0, an offset value of 0.8.

Maximum likelihood (ML) phylogenetic analyses using the nucleotide sequences were performed with RaxML-HPC2 BlackBox (Stamatakis *et al.*, 2008) through the CIPRES Science Gateway (Miller *et al.*, 2010). Bootstrapping was performed according to the default criteria on RaxML, where bootstrapping stops after 200-600 replicates. *Amborella trichopoda* genes were used as outgroup as follows: *AmtrAG* for the *AGAMOUS/SHATTERPROOF* analysis; *AmtrSPT* for the *SPATULA/ALCATRAZ* analysis; *AmtrRPL* for the *RPL analysis; AmtrFUL* for the *FUL* analysis. Trees were observed and edited using FigTree v1.4.3 and iTOL (https://itol.embl.de/itol.cgi). All sequences included in the phylogenetic analyses are listed in Supplementary Table S1.

Expression analyses by RT-PCR

To assess and compare the expression of *FUL, SHP, ALC, SPT, HEC1/2/3* and *RPL* in *C. nocturnum* and *B. suaveolens* we dissected carpels and fruits at different developmental stages previously selected based on our anatomical studies (Figs. 2A,3A). Total RNA was prepared from dissected carpels and fruits and whenever possible, seeds were removed. TRizol Reagent (Invitrogen, Waltham, MA, USA) was used for *C. nocturnum* and PureLink (Invitrogen, USA) was employed for *B. suaveolens.* RNA was re-suspended in 20 μl of RNAse free water. Samples were treated with DNAseI

(Roche, Basel, Switzerland) to remove genomic DNA contamination and quantified with a NanoDrop 2000 spectrophotometer (Thermo Scientific, Waltham, MA, USA). Three micrograms (3 μg) of RNA were used as a template for cDNA synthesis (SuperScript III RT, Invitrogen) using oligo dT primers. The cDNA was used undiluted for amplification reactions by RT-PCR. For *RPL* genes, primers were designed flanking both the BELL and the HD whenever possible. For *ALC/SPT* and *HEC1/2/3/IND* genes, primers were designed outside the conserved bHLH domain. For *FUL* and *SHP* primers were designed outside of the MADS and the K domains. All primers used were designed specifically for each paralog found in *C. nocturnum* and *B. suaveolens* (Supplementary Table S2). Each amplification reaction incorporated 9 μl of Econotaq (Lucigen, Middleton, WI, USA), 6 μl of nuclease-free water, 1 μl of BSA (bovine serum albumin)

(5 μg/ml), 1μl of Q solution (betaine 5 μg/μl), 1 μl of forward primer (10 mM), 1 μl of reverse primer (10 mM), and 1 μl of template cDNA, giving a total of 20 μl. Thermal cycling profiles followed an initial denaturation step (94 °C for 30 s), an annealing step (50-62 °C for 30 s) and an extension step with polymerase (72 °C for up to 1 min) repeated for 30-35 amplification cycles. *ACTIN* was used as a positive amplification control. PCR products were run on a 1.5% agarose gel stained with ethidium bromide and digitally photographed using a Whatman Biometra BioDoc Analyzer. For those genes whose expression was not detected in any developmental stage (for instance, *BrsuFUL2*) we repeated the RT-PCR varying the annealing temperature settings (5559°C). Finally, we compared the expression patterns obtained here with the data available for tomato on the eFP Browser (http://bar.utoronto.ca/efp2/Tomato/Tomato_eFPBrowser2.html) and data for *Nicotiana benthamiana* available in the Gene Expression ATLAS (http://sefapps02.qut.edu.au/atlas/tREX6.php).

Acknowledgements

This work was funded by the ExpoSeed (H2020 MSCA-RISE 2015-691109) EU grant, the Convocatoria Programáticas 2017-16302 and the Estrategia de Sostenibilidad 2018-2019, from the Universidad de Antioquia. NH-C was the recipient of an undergraduate Joven Investigador *fellowship at the Universidad de Antioquia. NP-M acknowledges the Dresden Junior Fellowship to visit the Technishe Universität Dresden and the Botanischer Garten TU Dresden, where many of the photographs for figure 1 were taken. The authors thank the members Plant Evo Devo group for support in laboratory protocols and two reviewers of this manuscript for their important comments.*

References

AVINO M, KRAMER EM, DONOHUE K, HAMMEL AJ, HALL JC (2012). Understanding the basis of a novel fruit type in Brassicaceae: conservation and deviation in expression patterns of six genes. *Evo Devo* 3: 1.

BEMER M, KARLOVA R, BALLESTER AR, TIKUNOV YM, BOVY AG, WOLTERS-ARTS M, ROSSETTO P d. B, ANGENENT GC, DE MAAGD RA (2012). The Tomato FRUITFULL Homologs TDR4/FUL1 and MBP7/FUL2 Regulate Ethylene-Independent Aspects of Fruit Ripening. *Plant Cell* 24: 4437–4451.

BOBROV AVFC, ROMANOV MS (2019). Morphogenesis of fruits and types of fruit of angiosperms. *Bot Lett* 166: 366–399.

BREMER B, ERIKSSON O (1992). Evolution of fruit characters and dispersal modes in the tropical family Rubiaceae. *Biol J Linn Soc* 47: 79–95.

CLAUSING G, MEYER K, RENNER SS (2000). Correlations among fruit traits and evolution of different fruits within Melastomataceae. *Bot J Linn Soc* 133: 303–326.

CORTÉS-FLORES J, ANDRESEN E, CORNEJO-TENORIO G, IBARRA-MANRÍQUEZ G (2013). Fruiting phenology of seed dispersal syndromes in a Mexican Neotropical temperate forest. *For Ecol Manage* 289: 445–454.

DUPIN J, SMITH SD (2018). Phylogenetics of Datureae (Solanaceae), including description of the new genus *Trompettia* and re-circumscription of the tribe. *Taxon* 67: 359–375.

FERRÁNDIZ C (2002). Regulation of fruit dehiscence in *Arabidopsis*. *J Exp Bot* 53: 2031–2038.

FERRÁNDIZ C, LILJEGREN SJ, YANOFSKY MF (2000). Negative regulation of the SHATTERPROOF genes by FRUITFULL during *Arabidopsis* fruit development. *Science* 289: 436–438.

FOURQUIN C, DEL CERRO C, VICTORIA FC, VIALETTE-GUIRAUD A, DE OLIVEIRA AC, FERRÁNDIZ C (2013). A change in SHATTERPROOF protein lies at the origin of a fruit morphological novelty and a new strategy for seed dispersal in Medicago genus. *Plant Physiol* 162: 907–917.

FOURQUIN C, FERRÁNDIZ C (2012). Functional analyses of AGAMOUS family members in Nicotiana benthamiana clarify the evolution of early and late roles of C-function genes in eudicots. *Plant J* 71: 990–1001.

GARCEAU DC, BATSON MK, PAN IL (2017). Variations on a theme in fruit development: the PLE lineage of MADS-box genes in tomato (TAGL1) and other species. *Planta* 246: 313–321.

GIRIN T, PAICU T, STEPHENSON P, FUENTES S, KORNER E, O'BRIEN M, SOREFAN K, WOOD TA, BALANZA V, FERRÁNDIZ C, SMYTH DR, OSTERGAARD L (2011). INDEHISCENT and SPATULA Interact to Specify Carpel and Valve Margin Tissue and Thus Promote Seed Dispersal in *Arabidopsis*. *Plant Cell* 23: 3641–3653.

GREMSKI K, DITTA G, YANOFSKY MF (2007). The HECATE genes regulate female reproductive tract development in *Arabidopsis Thaliana*. *Development* 134: 3593–3601.

GROSZMANN M, PAICU T, ALVAREZ JP, SWAIN SM, SMYTH DR (2011). SPATULA and ALCATRAZ, are partially redundant, functionally diverging bHLH genes required for *Arabidopsis* gynoecium and fruit development. *Plant J* 68: 816–829.

GU Q, FERRANDIZ C, YANOFSKY MF, MARTIENSSEN R (1998). The FRUITFULL MADSbox gene mediates cell differentiation during *Arabidopsis* fruit development. *Development* 125: 1509–1517.

HEISLER MGB, ATKINSON A, BYLSTRA YH, WALSH R, SMYTH DR (2001). SPATULA, a gene that controls development of carpel margin tissues in *Arabidopsis*, encodes a bHLH protein. *Development* 128: 1089–1098.

KATOH K (2002). MAFFT: a novel method for rapid multiple sequence alignment based on fast Fourier transform. *Nucleic Acids Res* 30: 3059–3066.

KAY P, GROSZMANN M, ROSS JJ, PARISH RW, SWAIN SM (2013). Modifications of a conserved regulatory network involving INDEHISCENT controls multiple aspects of reproductive tissue development in *Arabidopsis*. *New Phytol* 197: 73–87.

KNAPP S (2002). Tobacco to tomatoes: a phylogenetic perspective on fruit diversity in the Solanaceae. *J Exp Bot* 53: 2001–2022.

KONISHI S, IZAWA T, LIN SY, EBANA K, FUKUTA Y, SASAKI T, YANO M (2006). An SNP Caused Loss of Seed Shattering during Rice Domestication. *Science* 312: 1392–1396.

LARSSON A (2014). AliView: A fast and lightweight alignment viewer and editor for large datasets. *Bioinformatics* 30: 3276–3278.

LILJEGREN SJ, DITTA GS, ESHED Y, SAVIDGE B, BOWMANT JL, YANOFSKY MF (2000). SHATTERPROOF MADS-box genes control dispersal in *Arabidopsis*. *Nature* 404: 766–770.

LILJEGREN SJ, ROEDER AHK, KEMPIN SA, GREMSKI K, ØSTERGAARD L, GUIMIL S, REYES DK, YANOFSKY MF (2004). Control of fruit patterning in *Arabidopsis* by INDEHISCENT. *Cell* 116: 843–853.

MAHEEPALA DC, EMERLING CA, RAJEWSKI A, MACON J, STRAHL M, PABÓN-MORA N, LITT A (2019). Evolution and diversification of FRUITFULL genes in solanaceae. *Front Plant Sci* 10: 1–20.

MILLER MA, PFEIFFER W, SCHWARTZ T (2010). Creating the CIPRES Science Gateway for inference of large phylogenetic trees. *2010 Gatew Comput Environ Work GCE 2010*.

ORTIZ-RAMÍREZ CI, GIRALDO MA, FERRÁNDIZ C, PABÓN-MORA N (2019). Expression and function of the bHLH genes ALCATRAZ and SPATULA in selected Solanaceae species. *Plant J* 99: 686-702.

ORTIZ-RAMÍREZ CI, PLATA-ARBOLEDA S, PABÓN-MORA N (2018). Evolution of genes associated with gynoecium patterning and fruit development in Solanaceae. *Ann Bot* 121: 1211–1230.

PABÓN-MORA, N and LITT, A. (2011). Comparative anatomical and developmental analysis of dry and fleshy fruits of Solanaceae. *Am J Bot* 98: 1415–1436.

RAJANI S, SUNDARESAN V (2001). The *Arabidopsis* myc/bHLH gene alcatraz enables cell separation in fruit dehiscence. *Curr Biol* 11: 1914–1922.

ROEDER AHK, FERRÁNDIZ C, YANOFSKY MF (2003). The role of the REPLUMLESS Homeodomain protein in patterning the *Arabidopsis* Fruit. *Curr Biol* 13: 1630-1635.

ROEDER AHK, YANOFSKY MF (2006). *Fruit Development in Arabidopsis. Arabi-*

dopsis Book 4:e0075.

SCHUSTER C, GAILLOCHET C, LOHMANN JU (2015). *Arabidopsis* HECATE genes function in phytohormone control during gynoecium development. *Development* 142: 3343–3350.

SMYKAL P, GENNEN J, DE BODT S, RANGANATH V, MELZER S (2007). Flowering of strict photoperiodic Nicotiana varieties in non-inductive conditions by transgenic approaches. *Plant Mol Biol* 65: 233–242.

STAMATAKIS A, HOOVER P, ROUGEMONT J (2008). A rapid bootstrap algorithm for the RAxML web servers. *Syst Biol* 57: 758–771.

VREBALOV J, PAN IL, ARROYO AJM, MCQUINN R, CHUNG M, POOLE M, ROSE J, SEYMOUR G, GRANDILLO S, GIOVANNONI J, IRISH VF (2009). Fleshy Fruit Expansion and Ripening Are Regulated by the Tomato SHATTERPROOF Gene TAGL1. *Plant Cell* 21: 3041–3062.

ZUMAJO-CARDONA C, PABÓN-MORA N, AMBROSE BA (2018). Duplication and diversification of REPLUMLESS – A case study in the papaveraceae. *Front Plant Sci* 871: 1– 19.

Further Related Reading, published previously in the *Int. J. Dev. Biol.*

Instructive roles for hormones in plant development
David Alabadí, Miguel A. Blázquez, Juan Carbonell, Cristina Ferrándiz and Miguel A. Pérez-Amador
Int. J. Dev. Biol. (2009) 53: 1597-1608
https://doi.org/10.1387/ijdb.072423da

Genetic analysis of reproductive development in tomato
Rafael Lozano, Estela Giménez, Beatriz Cara, Juan Capel and Trinidad Angosto
Int. J. Dev. Biol. (2009) 53: 1635-1648
https://doi.org/10.1387/ijdb.072440rl

Historical perspectives on plant developmental biology
Mieke Van Lijsebettens and Marc Van Montagu
Int. J. Dev. Biol. (2005) 49: 453-465
http://www.intjdevbiol.com/web/paper/041927ml

Flower and fruit development in *Arabidopsis thaliana*
Pedro Robles and Soraya Pelaz
Int. J. Dev. Biol. (2005) 49: 633-643
http://www.intjdevbiol.com/web/paper/052020pr

Control of reproduction by Polycomb Group complexes in animals and plants
Anne-Elisabeth Guitton and Frederic Berger
Int. J. Dev. Biol. (2005) 49: 707-716
http://www.intjdevbiol.com/web/paper/051990ag

Flowering: a time for integration
François Parcy
Int. J. Dev. Biol. (2005) 49: 585-593
http://www.intjdevbiol.com/web/paper/041930fp

Long-range signalling in plant reproductive development
Paula Suárez-López
Int. J. Dev. Biol. (2005) 49: 761-771
http://www.intjdevbiol.com/web/paper/052002ps